Dynamic Model of an Integral-Cycle Controlled Single-Phase Induction Machine

Longya Xu, Member, IEEE

Department of Electrical Engineering
The Ohio State University
2015 Neil Avenue
Columbus, Ohio 43210

Abstract - A dynamic machine model of an integral-cycle controlled single-phase induction motor is derived by properly choosing a stationary d-q reference frame. By utilizing the derived model it is revealed that two types of capacitor connection to the machine windings are equivalent, and that the integral-cycle controlled single-phase induction machine switches its operation between two distinct modes. Comparison of simulated to tested results indicates that with the integral-cycle control, a complicated motor behavior may occur due to the irregular current waveform in operation.
KEYWORD: Induction Motor, Thyristor Controlled Motor, Electric Machine Modeling.

Introduction

In the fractional horsepower range, single-phase induction machines are very popular. It is estimated that production of single-phase induction machines exceeds that of polyphase machines by many times in the low horsepower range[1]. Single-phase induction machines are inherently suitable for single-phase power supplies, very simple in structure and rugged. Thus, cost-effective and highly reliable drives made with single phase machines can be expected. Two types of single-phase induction machines are most widely used: shaded-pole and permanent split capacitor (PSC) induction machines. The shaded-pole machines employ auxiliary short-circuit windings, known as "shade coils", to produce a quasi-rotating flux in the airgap. These types of machines are available only in the ratings of 1/20 hp or below because of their low efficiency. The permanent split capacitor (PSC) machines, on the other hand, refer to those in which the stator windings are split into two phases, and one phase winding is connected to a capacitor either permanently or in starting. The connection of a capacitor improves the performance of a single phase induction machine significantly. Therefore, the power rating of PSC machines is larger, and the application is more extensive than the shaded-pole machines.

To improve the performance of single-phase induction machines further, power electronic means have been employed increasingly to achieve adjustable speed operation in recent years, for instance in air conditioners and washing machines. Although many sophisticated control techniques such as field orientation or vector control techniques have been developed in the past decade for polyphase machines[2], the simple thyristor converters are employed very often for single-phase machine control. This is because the complexity and high cost of the newly developed controllers are not justifiable for single-phase induction machines with low-horsepower rating. Compared with the more advanced technology, a single-phase induction machine coupled with the thyristor converter, in effect, offers a far more cost-effective drive, satisfying most of the commercial and residential applications.

92 WM 057-0 EC A paper recommended and approved by the IEEE Electric Machinery Committee of the IEEE Power Engineering Society for presentation at the IEEE/PES 1992 Winter Meeting, New York, New York, January 26-30, 1992. Manuscript submitted August 30, 1991; made available for printing December 23, 1991.

We can categorize the simple control algorithms of a single-phase induction machine into two groups: the phase control and integral-cycle control methods. In the phase control method, the effective stator voltage is varied by means of TRIAC circuits that conduct for a portion of each half-cycle. As an alternative, the integral-cycle control method may be employed, using the antiparallel thyristors or TRIACs as static contactors and alternatively switching on and off the supply voltage for a number of cycles at a time [3] [4]. The effective stator voltage is varied by controlling the ratio of on-time to off-time, and speed fluctuations are avoided if the conducting and non-conducting intervals are short compared with the mechanical time constant of the system [4]. In addition to its simplicity in control and reasonable performance, the integral-cycle controlled induction motor offers other advantages. Less voltage distortion is produced on the ac supply, and less radio-frequency interference is propagated when integral-cycle systems are used rather than the phase -controlled regulators[5].

Although the combination of a single-phase induction machine with a thyristor based power supply configures the simplest and the least expensive drive in low horsepower application, the behavior of the system is not so simple as the configuration appears to be. In particular, with the integral-cycle control scheme the single-phase induction machine constantly changes operation modes, as will be made clear in the paper, resulting in complicated operational characteristics. Thus far, little attention has been directed to the dynamic analysis of the single-phase drive system with integral-cycle power control. In most cases, the analysis has been semi-intuitive with a modification of the conventional induction machine made to incorporate the difference created by the integral-cycle power supply. The control of the integral-cycle single-phase induction machine drives has been empirical. While some degree of speed control on such a type of system has been obtained, little attention has been paid to the transient behavior of the overall system. To this end, a scheme for modeling and simulation of the single-phase drive systems with integral-cycle control is clearly necessary. In this paper, a complete development of a suitable dynamic model is presented based on d-q transformation theory. The approach highlights the mode transition which occurs in the integral-cycle operation and clearly demonstrates the transient current waveforms in two different operation modes. Therefore, the analysis is also important to the understanding of induction machines with discontinuous excitations.

Machine Structure and System Configuration

The schematic configuration of an integral-cycle controlled single-phase induction machine is shown in Figure 1(a). The stator windings are split into two phases and wound 90° apart along the airgap space. As is well known, if the two sets of symmetric windings in space are excited by a two phase symmetrical AC voltage in time, a smooth rotating field will be produced. However, for single-phase excitation, a capacitor is connected in series with one phase winding, and both windings are excited by the single phase voltage. The rotor of the machine is of a cage style featuring a simple and rugged structure.

Two TRIACs are used in the system to function as a pair of electronically controlled switches so as to supply an integral-cycle controlled voltage to the induction machine. The two TRIACs are denoted as S1 and S2 in Figure 1. To command the machine to rotate in a clockwise direction, S2 is permanently open while S1 supplies integral-cycle voltage to the induction machine. Likewise,

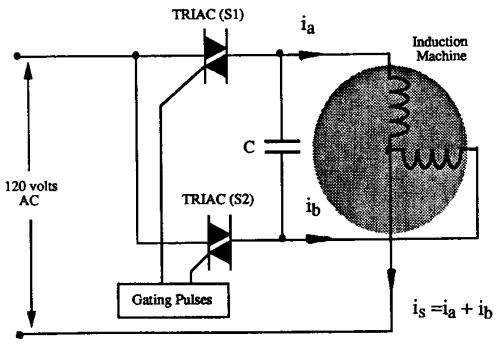

Figure 1(a). Integral-Cycle Controlled Single Phase Induction Machine Circuit

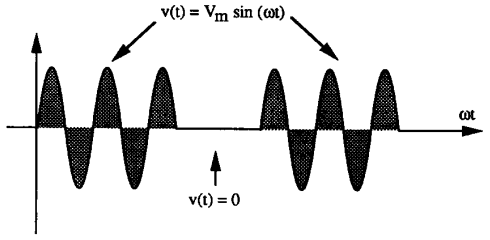

Figure 1(b). Integral-Cycle Controlled Single Phase Induction Machine Control Strategy

to command the machine to rotate in the other direction, S1 and S2 interchange their functions. Adjustable speed operation is obtainable for the system by controlling the ratio of the on-time to the off-time of the supply voltage. To illustrate the integral-cycle control, Figure 1(b) shows the voltage waveform imposed on the stator terminals. In general, the larger value of the ratio, the higher the speed of the motor. As the ratio reaches unity, the machine is operated with the full supply voltage. However, it is very important to realize that the induction machine exhibits complicated behavior under the integral-cycle control algorithm. For example, with the same load torque, the machine runs at 900 rpm when the supply voltage has a ratio of on-time/off-time at 5/3. However, when the the ratio of on-time/off-time increases to 5/2, the machine speed is reduced adversely to 725 rpm, a 25% drop from the previous case.

Operational Modes and Terminal Constraints

The operation of the system in Figure 1 can be characterized in four modes, two in each rotating direction. The terminal constraints imposed by the TRIACs on the motor are as follows.

Forward Rotating:

Mode I (S1 on and S2 off)

$$\begin{aligned} V_s &= V_a \\ V_a &= V_b + V_c \\ i_s &= i_a + i_b \end{aligned} \qquad (1.a)$$

Mode II (S1 and S2 off)

$$\begin{aligned} V_a &= V_b + V_c \\ i_a + i_b &= 0 \end{aligned} \qquad (1.b)$$

Reverse Rotating:

Mode III (S2 on and S1 off)

$$\begin{aligned} V_s &= V_b \\ V_a &= V_b + V_c \\ i_s &= i_a + i_b \end{aligned} \qquad (2.a)$$

Mode IV (S1 and S2 off)

$$\begin{aligned} V_a &= V_b + V_c \\ i_a + i_b &= 0 \end{aligned} \qquad (2.b)$$

Note that the constraints in Mode II and Mode IV are the same as far as the electrical variables are concerned. This suggests that only one mode needs to be analyzed between Modes II and IV for the electrical transients of the system. Furthermore, the functions of the two phase windings are symmetric in the forward and reverse rotating modes as indicated by the constraints in Mode I and Mode III. This suggests that only one mode needs to be analyzed between Mode I and Mode III. Based on these observations, Modes I and II are chosen as the fundamental modes to be studied in this paper, that is, the one in which both TRIACs are open and the other in which only one TRIAC remains open. Since thyristor type devices are used in the system, the transition from Mode I to Mode II occurs when the current of the TRIAC is crossing zero upon receiving a turn-off command.

In spite of the reduced number of modes, it is still difficult to model the transition from one mode to the other. In particular, when the thyristor commutes from the ON state to OFF state or vise versa, the order of the system changes. The variation of the system order due to the mode transition will be discussed later.

D-Q Modeling in Stationary Reference Frame

To avoid the difficulties in dynamic modeling of the system, we have chosen to formulate the motor equations in a proper stationary d-q reference frame, as shown in Figure 2.

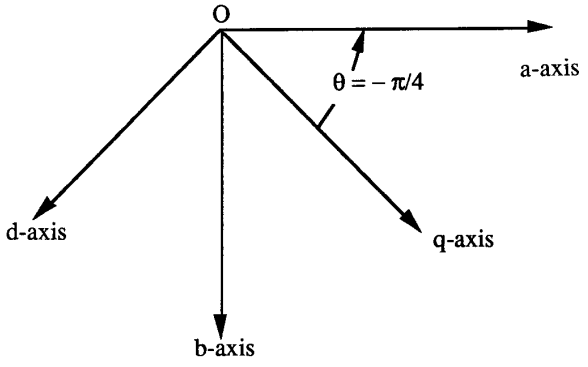

Figure 2. Relationships of the Original *a-b* Reference Frame to the Transformed *d-q* Reference Frame

As shown in the figure, the original system is denoted as the *a-b* system, while the transformed system is denoted as the *d-q* system. The relationships between the variables in the original a-b system and those in the d-q system are specified by

$$\begin{pmatrix} V_{qs} \\ V_{ds} \end{pmatrix} = \frac{\sqrt{2}}{2} \begin{pmatrix} 1 & 1 \\ -1 & 1 \end{pmatrix} \begin{pmatrix} V_a \\ V_b \end{pmatrix} \qquad (3)$$

Because the transformation matrix is constant, the new reference frame is relatively stationary compared to the original *a-b* system with 45° angle displacement.

The transformation may be interpreted alternatively. If the original stator windings are replaced physically by a set of new windings located along the d- and q-axes and excited by v_{ds} and v_{qs}, the same magnetic field will be produced along the airgap. A more important aspect of the transformation concerns the terminal constraints. Under the transformation, the constraints (1.a) in Mode I (S1 on) become

$$V_{ds} = \frac{\sqrt{2}}{2}(-V_a + V_b) = \frac{\sqrt{2}}{2}(-V_c) \qquad (4.a)$$

$$V_{qs} = \frac{\sqrt{2}}{2}(V_a + V_b) = \frac{\sqrt{2}}{2}(2\,V_s - V_c) \qquad (4.b)$$

$$i_s = i_{qs} = i_{ds} + i_c \qquad (4.c)$$

In the case of Mode II constrained by (1.b), the transformed constraints (both switches are off) are

$$V_{ds} = \frac{\sqrt{2}}{2}(-V_a + V_b) = \frac{\sqrt{2}}{2}(-V_c) \qquad (5.a)$$

$$i_{qs} = 0 \qquad (5.b)$$

For the convenience of comparison, a circuit describing the two fundamental modes of the single-phase induction machine in terms of *a-b* variables is given in Figure 3(a). From Equations (4) and (5), an equivalent stator arrangement replacing the original circuit of Fig. 3(a) can be obtained as shown in Fig. 3(b). Clearly we can see that the equivalent capacitor C is now in parallel with the winding located on d-axis. In addition, when the TRIACs are open, the winding located on the q-axis is open-circuited.

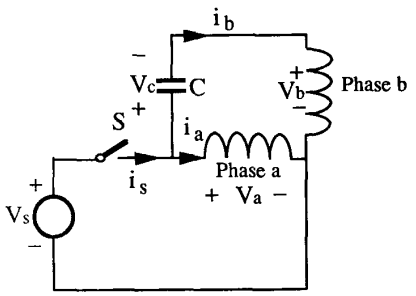

Figure 3(a). Original Stator Winding Connection to the TRIAC and Capacitor

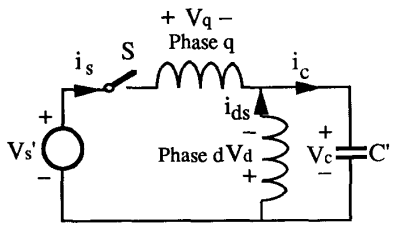

Figure 3(b). Transformed Stator Winding Connection to the TRIAC and Capacitor

It is difficult to identify the operational characteristics of the machine from the original description in terms of *a-b* variables. However, the equivalent circuit in the transformed reference frame in terms of *d-q* variables gives a straightforward description and provides insights into the understanding of the system. For example, in the transformed equivalent circuit, it is quite clear that when the switch is off, the induction machine has only one phase stator winding closed and, thus, the induction machine is truly in single-phase operation. During this period, the capacitor shorts the active phase winding at the terminals and no energy enters the system. Therefore, the machine is running on the energy stored in the capacitor and in the magnetizing inductor. On the other hand, when the switch is on, both phases are energized with one phase winding shunted by the capacitor. In this case, the current through the winding shunted by the capacitor is different from that through the other winding. From there, a phase angle between the two currents is created, and the machine operation is more similar to that of a two-phase induction machine. Consequently, by turning the switch on and off, the induction machine changes its operational characteristics between the two different modes repetitively.

It is also very interesting to notice the connection of the capacitor with respect to the windings in the original and transformed circuits respectively. In the original system, the capacitor is connected in series with one winding, while in the transformed system, the capacitor is connected in parallel with one winding. According to the equivalence of the transformation, there is no difference between these two connections as far as the terminal characteristics of the system are concerned. Practically, however, with the series connection the motor can be easily controlled to operate in both directions with a minimum number of thyristors.

Nevertheless, the transformed model facilitates the analysis of the machine. Particularly, in Mode II both phases of the windings are disconnected from the power supply. If the original circuit is applied in the analysis of the machine, the capacitor would couple with both windings, complicating the system equations. However, in the transformed circuit the capacitor couples with only one stator winding, simplifying the circuit and indicating immediately that the order of the machine equations is reduced.

Dynamic Equations of the System

Taking the capacitor voltage v_c as an additional state variable, the dynamic equations of the motor in terms of flux linkages λ_{qs}, λ_{ds}, λ_{qr}, λ_{dr}, and rotor speed ω_r are as follows (all notations retain their conventional meanings):

$$\frac{d\lambda_{ds}}{dt} = v_{ds} - r_s i_{ds} \qquad (6)$$

$$\frac{d\lambda_{qs}}{dt} = v_{qs} - r_s i_{qs} \qquad (7)$$

$$\frac{d\lambda_{dr}}{dt} = -\frac{2}{p}\omega_r \lambda_{qr} - r_r i_{dr} \qquad (8)$$

$$\frac{d\lambda_{qr}}{dt} = \frac{2}{p}\omega_r \lambda_{dr} - r_r i_{qr} \qquad (9)$$

$$\frac{dv_c}{dt} = \frac{1}{C} i_c \qquad (10)$$

$$i_c = \sqrt{2}\,(i_{ds} + i_{qs}) \qquad (11)$$

$$i_{ds} = -\frac{L_{mp}}{L_1 L_2}\lambda_{dr} + \frac{L_1 - L_{mp}}{L_1^2}\lambda_{ds} \qquad (12)$$

$$i_{qs} = -\frac{L_{mp}}{L_1 L_2}\lambda_{qr} + \frac{L_1 - L_{mp}}{L_1^2}\lambda_{qs} \qquad (13)$$

$$i_{dr} = -\frac{L_{mp}}{L_1 L_2}\lambda_{ds} + \frac{L_2 - L_{mp}}{L_2^2}\lambda_{dr} \qquad (14$$

$$i_{qr} = -\frac{L_{mp}}{L_1 L_2}\lambda_{qs} + \frac{L_2 - L_{mp}}{L_2^2}\lambda_{qr} \qquad (15)$$

where $$L_{mp} = \frac{1}{\frac{1}{L_1} + \frac{1}{L_2} + \frac{1}{L_m}}\,.$$

$$\frac{d\omega_r}{dt} = \frac{1}{J}\frac{p}{2}(T_e - T_l) - \frac{D}{J}\omega_r \qquad (16)$$

$$T_e = \frac{3}{2}\frac{p}{2} L_m (i_{dr} i_{qs} - i_{qr} i_{ds}) \qquad (17)$$

Equations (6) through (17), together with the load characteristic $T_l(t)$ as provided by the user, are the complete

description of the single-phase induction machine. These equations form the kernel of the dynamic simulation of the system. Note that Equations (6) through (10) can be written intuitively according to the suggested equivalent circuit shown in Figure 3(b). The derivation of the current equations in terms of flux linkages is given in Appendix. To find the transient response of the system with the integral-cycle controlled voltage, we must solve Equations (6) through (17) simultaneously. Furthermore, according to Equations (6) through (17), a transient equivalent circuit can be suggested as shown in Figure 4.

A more detailed explanation can be given as follows regarding the order reduction of the dynamic equations when the switch is off. It should be noted that during the interval when the switch is off v_{qs} is a system response instead of a specified excitation as in the case of the switch being closed. In addition, because i_{qs} is zero, the stator flux linkage λ_{qs} and the airgap flux linkage λ_{qm} are identical and one variable is removed from the system equations. Thus, Equations (7) and (13) can be eliminated from the system dynamic equations, resulting in a reduced order model. The reduction of the system order merits a careful treatment in the simulation programming.

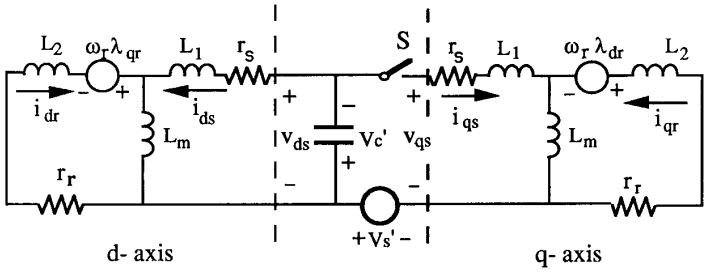

Figure 4. Equivalent Circuit for the Dynamic Simulation

Comparison of the Simulated and Experimental Results

A computer simulation program has been written based on the the dynamic equations derived in the last section, and several important investigations have been conducted. In order to validate the computer model, tests were made on a prototype 1/3 hp machine. This machine is rated at 120 volts. The specifications of the machine are listed in Table 1.

The steady-state speed response with excitation of 7 half-line-cycles on and 3 off is shown in Figure 5. The load torque applied in the simulation is 4.4 lb-in. The tested steady-state speed under the same conditions is 1180 rpm. The simulated results correlated to the tested results very well. Large torque ripple is observed from the simulated torque response. The torque ripple is due to the discontinuous excitation of the integral-cycle controlled voltage. During the off-time of the supply voltage, not only the stored energy in the electromagnetic field is reduced, the kinetic energy is also reduced. This is made evident by the slight reduction of the rotor

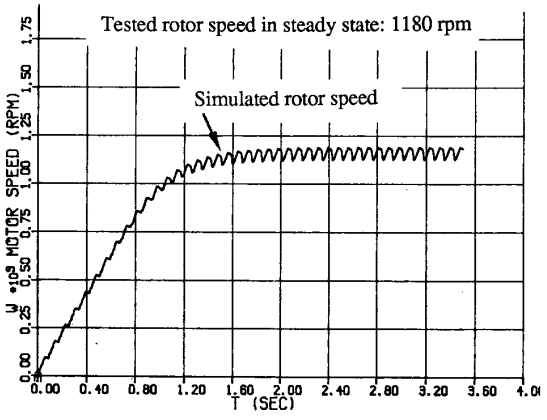

Figure 5. Speed Response of the Integral-Cycle Controlled Single-Phase Induction Machine

mechanical speed as shown in the figure. However, the high frequency torque ripple is filtered out by the rotor inertia, and the speed ripple is around 3% of the command speed as shown by the simulation.

More interesting simulation results are shown for the speed response by changing the on-time to off-time ratio of the terminal voltage for speed control. As shown in Figure 6, when the ratio of the on-time to off-time is controlled at 5/3, the simulated steady-state speed is 900 rpm. If the on/off ratio increase to 5/2, the speed is expected to increase. However, the rotor speed drops adversely to 725 rpm, poorer than expected. In both cases, the load torque is the same, 9 in-lb. These simulation results are also verified by the test results. This unproportional speed variation with respect to the voltage on/off ratio may be explained by the distorted current waveforms under the integral-cycle control algorithm. It is extremely important to realize that large value of subharmonic voltage components can be generated by the integral-cycle control scheme. Because it is not easy to drop subharmonic voltages by the machine inductance, the subharmonic currents may sometimes dominate the behavior of the machine.

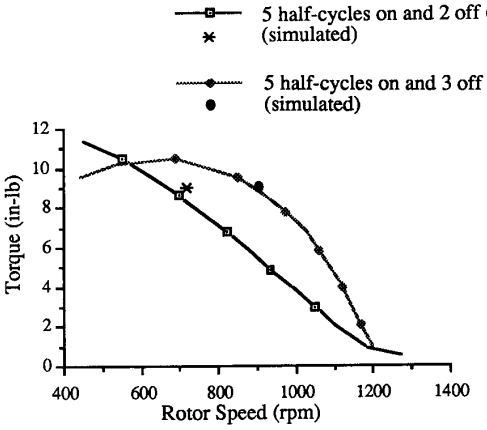

Figure 6. Unproportional Speed Reaponse with Different Integral-Cycle Ratios

Perhaps, it is more instructive to investigate the current waveforms of the integral-cycle controlled single-phase induction machine. Figure 7 shows the two phase stator currents, i_a and i_b,

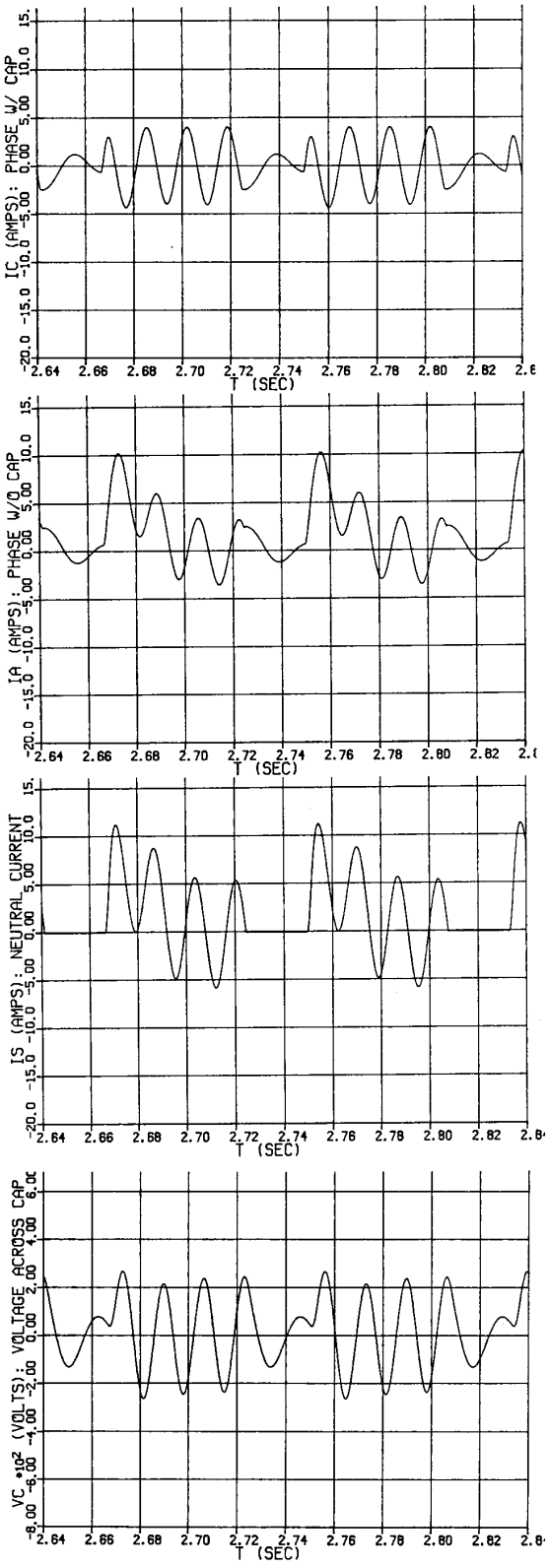

Figure 7. Simulated Current and Voltage Waveforms

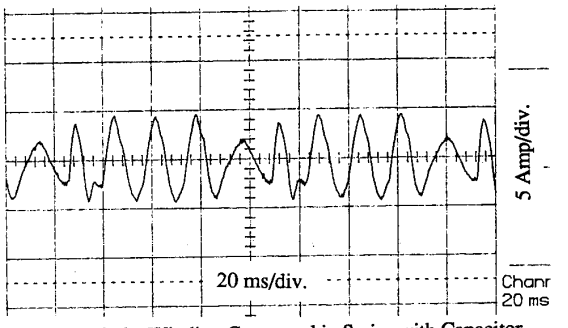

Current through the Winding Connected in Series with Capacitor

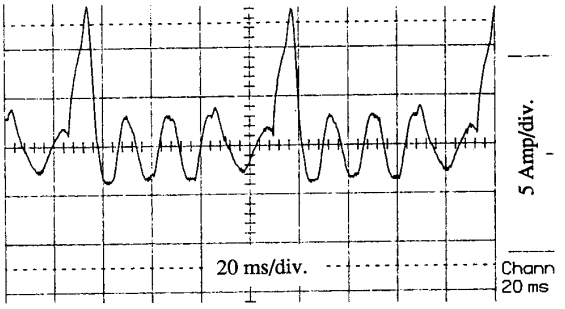

Current through the Winding without Connection to Capacitor

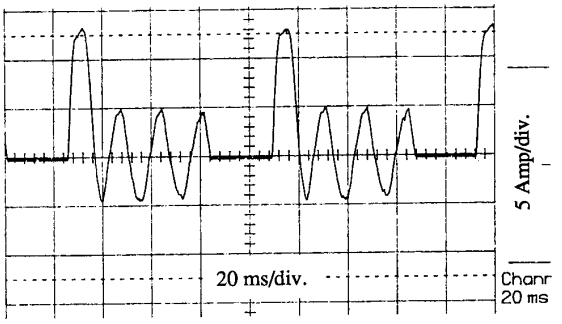

Current through Neutral Point

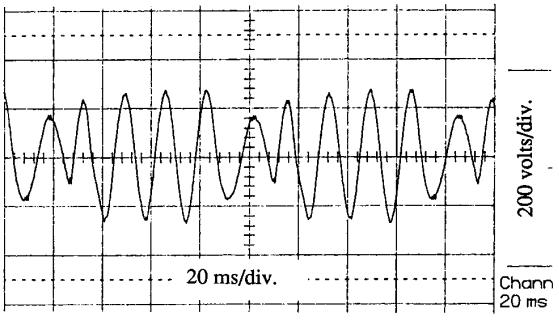

Voltage Across Capacitor

Figure 8. Current and Voltage Waveforms from Experiment

the current i_s through the returning path, and the voltage v_c across the capacitor obtained from the computer simulation. The TRIAC is switched with 7 half-line-cycles on and 3 off. Figure 8 shows the corresponding current and voltage waveforms measured from the tests. It can be seen that the currents and voltage predicted by the dynamic model agree very well with those measured from the experiment. It is also noticeable that the phase currents continue at each mode transition and the currents are substantial even though the machine is completely decoupled from the supply voltage. While the current through the returning path is identically zero when the TRIAC is off, the currents through the stator windings circulate via the capacitor. As discussed previously, in this case the machine runs on the energy stored in the capacitor as well as in the magnetic field of machine. The correctly simulated current and voltage waveforms give further explanations on the complicated speed behavior of the single-phase induction machine with the integral-cycle contolled voltage.

Conclusions

A complete dynamic model has been developed for an integral-cycle controlled single-phase induction machine by properly choosing a stationary d-q reference frame. It is shown that there are two types of equivalent capacitor connections for the single-phase induction machines. It is also shown that when an integral-cycle controlled voltage is applied, a single-phase induction machine switches its operational modes alternatively between the two circuits with different order. A computer investigation of the integral-cycle controlled single phase induction machine has been conducted based on the dynamic model. The transient responses from the simulation are in good agreement with those obtained from the experimental testing. This dynamic model has been proven very useful in predicting the complicated behavior of the integral-cycle controlled single-phase induction machines and in understanding of the induction machines with discontinuous excitations.

Table 1

Specifications of the experimental single-phase induction machine:

Power rating:	1/3 hp
Rated speed:	1600 rpm
Full load torque:	13 in-lb
Rated voltage:	120 volts
Frequency:	60 Hz
Stator winding resistance r_1:	4.5 ohms
Rotor cage resistance r_2:	18 ohms
Total leakage inductance $x_1 + x_2$:	6.07 ohms
Magnetising inductance x_m:	63.50 ohms
capacitor:	45μf
Triac:	MAC218A8

References:

[1] C. G. Veinott, "Theory and Design of Small Induction Motors", Book, McGraw-Hill Book Company Inc., New Yok, 1975

[2] T. A. Lipo, "Recent Progress in the Development of Solid-State AC Motor Drives", IEEE Transactions on Power Electronics, April, 1988, pp. 105-117

[3] J. M. D. Murphy and F. G. Turnbull, "Power Electronic Control of AC Motors", Book, Pergamon Press, Oxford, 1988

[4] William Shepherd, "Thyristor Control of AC Circuits", Book, Bradford University Press, London, 1975

[5] B.W. Lingard, R. W. Johson, W. Shepherd,"Analysis of Thyristor Controlled Single-Phase Loads with Integal-Cycle Triggering ", Proc. IEE, Vol. 117,1970, pp. 168-176

Appendix

The stator and rotor flux linkages of a two phase induction machine are produced by the stator and rotor currents as shown by the following equations in terms of *d-q* variables.

$$\lambda_{qs} = L_1 i_{qs} + L_m (i_{qs} + i_{qr}) \quad \text{(A-1)}$$

$$\lambda_{ds} = L_1 i_{ds} + L_m (i_{ds} + i_{dr}) \quad \text{(A-2)}$$

$$\lambda_{qr} = L_2 i_{qr} + L_m (i_{qs} + i_{qr}) \quad \text{(A-3)}$$

$$\lambda_{dr} = L_2 i_{dr} + L_m (i_{ds} + i_{dr}) \quad \text{(A-4)}$$

where the L_1 and L_2 are the leakage inductances of the stator and rotor windings respectively. L_m is the mutual inductance between rotor and stator windings. The parameters and variables on the rotor side have been referred to the stator side.

Equations A-1 through A-4 can be solved for the currents i_{qs}, i_{ds}, i_{qr}, and i_{dr} in terms of flux linkages. The following are obtained:

$$i_{ds} = -\frac{L_{mp}}{L_1 L_2}\lambda_{dr} + \frac{L_1 - L_{mp}}{L_1^2}\lambda_{ds} \quad \text{(A-5)}$$

$$i_{qs} = -\frac{L_{mp}}{L_1 L_2}\lambda_{qr} + \frac{L_1 - L_{mp}}{L_1^2}\lambda_{qs} \quad \text{(A-6)}$$

$$i_{dr} = -\frac{L_{mp}}{L_1 L_2}\lambda_{ds} + \frac{L_2 - L_{mp}}{L_2^2}\lambda_{dr} \quad \text{(A-7)}$$

$$i_{qr} = -\frac{L_{mp}}{L_1 L_2}\lambda_{qs} + \frac{L_2 - L_{mp}}{L_2^2}\lambda_{qr} \quad \text{(A-8)}$$

where $$L_{mp} = \frac{1}{\frac{1}{L_1} + \frac{1}{L_2} + \frac{1}{L_m}} . \quad \text{(A-9)}$$

Equations (A-1) through (A-9) can be applied in induction machine modeling using flux linkage as the state variables.

Longya Xu was born in Hunan, China. He graduated from Shangtan Institute of Electrical Engineering in 1970. He received the B.E.E. from Hunan University, China, in 1982, and M.S. and Ph. D. from the University of Wisconsin, Madison, in 1986 and 1990.

From 1971-1978 he participated in 150 kvA synchronous machine design, manufacturing and testing in China. From 1982-1984, he worked as a researcher for linear electric machines in the Institute of Electrical Engineering, Sinica Academia of China. Since he came to the U.S., he has served as a consultant to several industry companies including Raytheon Co., US Wind Power Co., Pacific Scientific Co., and Unique Mobility Inc. for various industrial concerns. He joined the Department of Electrical Engineering at the Ohio State University in 1990, where he is presently an Assistant Professor. Dr. Xu received the 1990 First Prize Paper Award in the Industry Drive Committee, IEEE/IAS. His research and teaching interests include dynamic modeling and converter optimized design of electrical machines and drive systems.

Discussion

M. Akbaba, (College of Engineering, The University of Bahrain, State of Bahtain): In figure 6 of the paper the author has compared the torque-speed characteristic of the machine for two different values of the duty cycle, and he showed that the torque resulting from a longer duty cycle, which produces larger average voltage, is less then the torque resulting from a relatively shorter duty cycle, which produces relatively smaller average voltage. He have pointed out that this unexpected result may be explained by the distorted current wave forms.

The low value of the torque at relatively high voltage may be explained by the following two reasons, where both are related to the saturation of the machine core at higher voltages:

a) At higher voltages the main winding flux path may saturate and this may cause a significant decrease in the self inductance of the main winding. In such a case the phase difference between the supply voltage and the main winding as well as the phase difference between the main winding and the starting winding will narrow down. As a result of this the machine will produce weaker rotating field and this will result in a reduced torque.
b) The saturation of the core will cause distortion in the current wave forms as pointed out by the author and shown in the figure 8 of the paper. Therefore, current harmonics resulted from saturation will produce harmonic torques. In this case some of the lower order harmonic torques may oppose to the fundamental torque and the total torque may be reduced.

Perhaps the author would like to comment on these points.

Manuscript received February 21, 1992.

LONGYA XU: I appreciate the comments supplied by Mr. Mehmet Akbaba, particularly that regarding the current distortion caused by core saturation. Indeed, saturation affects the current distortion. However, we should realize that saturation is closely related to the instantaneous voltage applied. Hence, it is believed that saturation will give nearly the same effect to the machine in both cases in Fig. 6 since the magnitude of the supply voltage remains the same for both cases. The "higher voltages" referred in the discussion actually are the averaging voltages produced by the higher on/off ratio of the integral cycles. Therefore, the "higher voltages" defined by the higher on/off ratios can not explain how the machine is saturated differently in the two cases.

The switching pattern seemed to impact the current distortion significantly. In particular, when the switching on/off ratio changes from 3/2 to 3/2, not only the averaging voltage changes, but more significantly, the symmetry of the current waveform changes resulting in a spectrum of very different harmonic components from that in the previous case. In fact, the unproportional speed responses under the voltages with these two different on/off ratios have been simulated successfully by the dynamic model in the paper where saturation is not included.

The change of the current symmetry can be understood by observing the current waveforms in Figure 8. For example, if the on/off ratio is 7/3 as shown in the figure, the peaky current is always positive and the current repeats its pattern every 10 half-cycles. However, when the on/off ratio changes to 6/3, the peaky current flips to positive and negative alternatively, and the current repeats its pattern every 18 half-cycles. It is obvious that the switching pattern impacts the harmonic components of the current and, thus, the torque-speed characteristics very much.

Manuscript received April 6, 1992.